

Design of Broadband Implantable Antenna for Biomedical Application

Ching-Fang Tseng*, Bo-Zhong Huang, Wen-Chieh Chuang

Department of Electronic Engineering, National United University, Taiwan
cftseng@nuu.edu.tw, berg0308@gmail.com, U0022105@smail.nuu.edu.tw

Abstract

A broadband implantable antenna is presented for the biomedical implantable system applications. The proposed antenna adopts a spiral monopole structure to realize the purpose of miniaturization size. The total size of the antenna including the biocompatible superstrates is $15 \times 15 \times 1.42$ mm³ operating frequency at 402 MHz. The effects of some design parameters on performance of proposed antenna are discussed. The simulated and measured in skin-mimicking gel show that the broad bandwidths of 150 MHz (310–460 MHz) and 260 MHz (280–540 MHz) at return loss of 10 dB can be achieved covering the entire Medical Device Radiocommunications Service (MedRadio) and Industrial Scientific Medical (ISM, 433–438 MHz) bands, respectively. The broadband implantable antenna performs an omnidirectional pattern, showing a good candidate for biomedical implantable systems application.

Keywords: Implantable antenna, Medical Device Radiocommunications Service (MedRadio), Industrial Scientific Medical (ISM), Broadband antenna

1 Introduction

Over the past few decades, implantable medical devices (IMDs) have attracted the attention of researchers for its applications in collecting physiological data and health monitoring of the patients toward wireless communication with the receiver equipment outside the human body. IMDs are used for many biomedical telemetry applications such as glucose monitoring, hyperthermia for cancer treatment, biomedical sensors, cardiac pacemakers, and capsule endoscopy [1-4]. The IMD is composed of many components in which an implantable antenna is the most crucial component because the transmission and reception of the signal must rely on the antenna working. The dielectric properties of human tissue are change with gender, age, weight, etc. which influence the impedance matching and stability of the resonant performance of an implantable antenna. Moreover, the size limits, human safety regulations and high data-rate transmission also are the essential requirements for an antenna inside the body, that make the implanted antenna designs challenging [5-7]. The available bandwidth of the implantable antenna is an important parameter to maximize the system performance with a high data rate; for instance, visual

prosthesis and multichannel neural recording systems need sufficient bandwidth to satisfy a requirement of high data rate up to 10 Mb/s [8].

The Medical Device Radio Communication Service (MedRadio, 401–406, 413–419, 426–432, 438–444, and 451–457 MHz), the Wireless Medical Telemetry Service (WMTS, 608–614, 1395–1400, and 1427–1432 MHz), and the Industrial Scientific Medical (ISM) (433–438 MHz; 886–906 MHz; 2.4–2.48 GHz; and 5.725–5.875 GHz) are approved and currently used in different medical implant applications [9-19]. At lower frequencies, implanted antennas have the better signal propagation characteristics inside the human body, but they have relative bigger sizes compared with that used in higher frequencies.

Base on signal propagation characteristics, the proposed implantable is designed to use at around 400 MHz medical implant applications in this paper. Moreover, we attempt to design an implantable antenna with compact size, broad operation bandwidth and high data rate that is capable of monitoring patient physiological data wirelessly in real time for various biomedical telemetry applications. A spiral monopole resonator with an inverse I-shaped ground plane is used to satisfy the implanted space limit. Owing to the strong coupling happens between both, the best impedance matching and broadband performance can be obtained by tuning their size to catch more signal energy for achieving wideband communication with a high data rate. Detail results of the proposed antenna design and experimental results are presented and discussed.

2 Antenna Design

Figure 1 displays the precise geometry of the proposed broadband bioimplantable antenna fed by 50Ω microstrip line. A spiral monopole resonator to realize the purpose of miniaturization size is printed on one side of a 0.8 mm thickness FR4 substrate with $\epsilon_r = 4.4$ and loss tangent $\tan\delta = 0.02$, and an inverse I-shaped ground plane on the other side as well. For the superstrate, an Al₂O₃ with a thickness of 0.64 mm, $\epsilon_r = 9.8$ and loss tangent $\tan\delta = 0.0087$ is laid over the spiral monopole resonator to preserve its biocompatibility and robustness, as shown in Figure 1(b). The whole antenna dimension is $15 \times 15 \times 1.42$ mm³. The detailed parameters of the proposed implantable antenna are presented in Figure 1(a). By tuning W_1 , W_2 , GW and GL , the broadband performance can be achieved for MedRadio application. Because the proposed antenna is expected to embedded inside

the human skin, the surrounding media is considered in simulated and measured processes. A simplified rectangular biological tissue model with dimension of $60 \times 60 \times 20 \text{ mm}^3$ is adopted to simulate and the proposed antenna is placed at 4 mm in depth inside the model [11]. The appropriate real skin recipe for skin-mimicking gel at 402 MHz consists of 55.92% sugar, 2.53% NaCl salt, and 41.55% deionized water to form 100 ml solution and then 1 g agarose is added in the solution, which are used in [17] as a human skin model. The dielectric constant and conductivity of skin-mimicking gel at 402 MHz are 46.37 and 1.22 S/m, respectively.

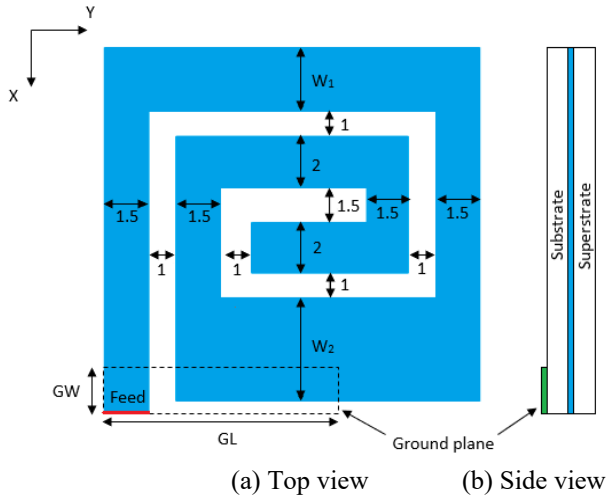


Figure 1. The proposed bioimplantable antenna geometry: (a) Top view and (b) Side view

3 Results and Discussions

By correct choice of W_1 , W_2 , GL and GW , the good impedance mating and the suitable operating frequency for implantable biotelemetry systems application. The simulated S_{11} characteristics of the proposed bioimplantable antenna with different dimensions (W_1 and W_2) of the spiral monopole resonator are plotted in Figure 2 and Figure 3. It can be seen and the resonant frequencies increase simultaneously as W_1 and W_2 increase from 1.3 to 2.2 mm and 1 to 4 mm, respectively. Moreover, the best bandwidth performance can be obtained at $W_1 = 1.9 \text{ mm}$ and $W_2 = 4 \text{ mm}$. To investigated the effects of the ground plane's size on the impedance characteristics of the proposed antenna, the simulated S_{11} with various GL and GW are shown in Figure 4 and Figure 5. Because of the strong fringing fields of the vertically placed strip resonator and ground plane, the proposed antenna produces easily nearby coupling [20]. Hence, the impedance matching is sensitive to the dimensions of GL and GW in the proposed structure. As shown in Figure 4 and Figure 5, the impedance matching is improved effectively by decreasing GL and GW and the optimized size of the ground plane is $GL = 9 \text{ mm}$ and $GW = 1.5 \text{ mm}$. The current path length (L) which follows around the white dash path of Figure 1(a) is introduced to describe above S_{11} characteristics. The estimated current path length of the proposed monopole spiral resonator is about $93.75 - 3W_1 - 2W_2 - GW$, while the change of the corresponding quarter wavelength resonance frequencies (f_r) of the proposed antenna with different W_1 , W_2 and GW are presented in Table 1. It can be clearly seen that the proposed antenna provides

resonance characteristics at about 0.4 GHz for all W_1 , W_2 and GW values. The resonance frequency moves to high frequency with increasing W_1 , W_2 and GW because of the current length reduction. As observed from Table 1, the calculated shift frequency level (Δf) is more in evidence by tuning W_2 , which is harmonized with the simulated S_{11} result. In addition, it can not only explain that why the resonance frequency remains unchanged with varying GL through analysis of the current path length but also understand how the mechanism of resonant mode excites.

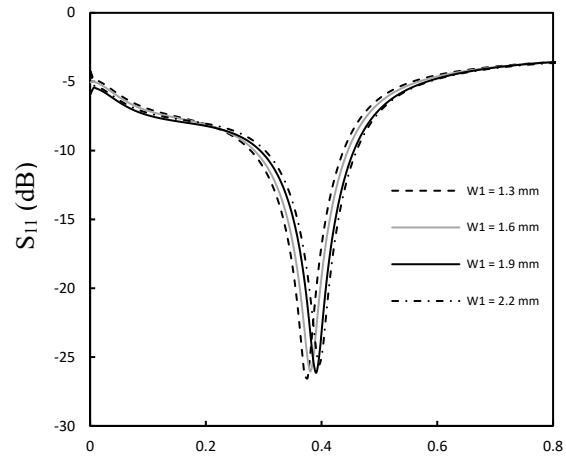


Figure 2. Simulated S_{11} for the proposed implantable antenna for different W_1 values with fixed values $W_2 = 4 \text{ mm}$, $GL = 9 \text{ mm}$ and $GW = 1.5 \text{ mm}$

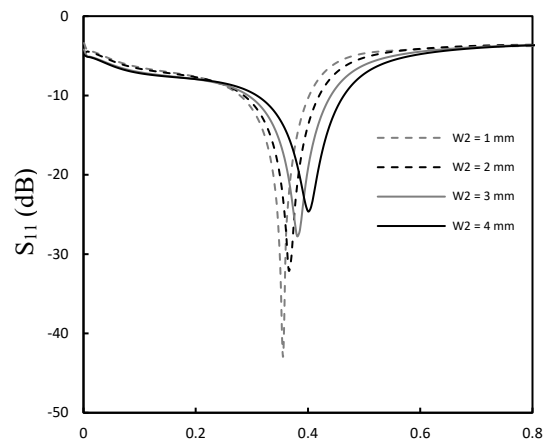


Figure 3. Simulated S_{11} for the proposed implantable antenna for different W_2 values with fixed values $W_1 = 1.9 \text{ mm}$, $GL = 9 \text{ mm}$ and $GW = 1.5 \text{ mm}$

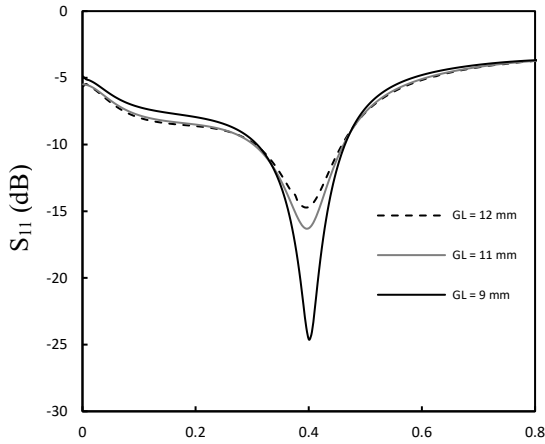


Figure 4. Simulated S_{11} for the proposed implantable antenna for different GL values with fixed values $W_1 = 1.9$ mm, $W_2 = 4$ mm and $GW = 1.5$ mm

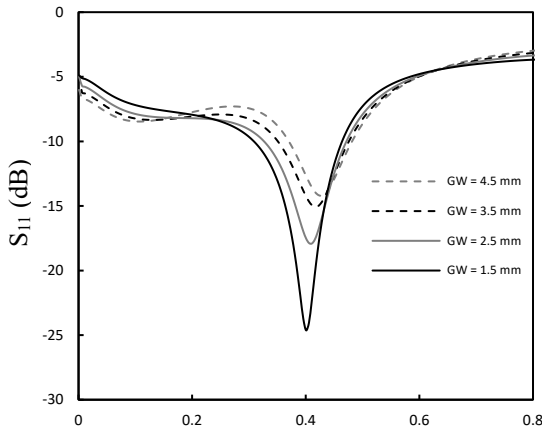


Figure 5. Simulated S_{11} for the proposed implantable antenna for different GW values with fixed values $W_1 = 1.9$ mm, $W_2 = 4$ mm and $GL = 9$ mm

Table 1. The change of resonance frequency (f_r), current path length (L) and calculated shift frequency (Δf) of the proposed antenna with different W_1 , W_2 and GW values

| W_1 (mm) | W_2 (mm) | GW (mm) | L (mm) | f_r (MHz) | Δf (MHz) |
|---------------|---------------|------------|-----------|----------------|---------------------|
| 1.3 | | | 80.35 | 444.99 | - |
| 1.6 | 4 | 1.5 | 79.45 | 450.03 | 5.04 |
| 1.9 | | | 78.55 | 455.19 | 5.16 |
| 2.2 | | | 77.65 | 460.46 | 5.27 |
| | 1 | | 84.55 | 422.88 | - |
| 1.9 | 2 | 1.5 | 82.55 | 433.13 | 10.25 |
| | 3 | | 80.55 | 443.88 | 10.75 |
| | 4 | | 78.55 | 455.19 | 11.31 |
| | | 1.5 | 78.55 | 455.19 | - |
| 1.9 | 4 | 2.5 | 77.55 | 461.06 | 5.87 |
| | | 3.5 | 76.55 | 467.08 | 6.02 |
| | | 4.5 | 75.55 | 473.26 | 6.18 |

The proposed antenna was implanted into skin-mimicking gel to emulate human skin and the simulated and measured S_{11} results are shown in Figure 6. It can be observed that there exists a discrepancy between simulated and measured results.

Because of the inaccurate material allocation proportion, the skin-mimicking gel has the slightly lower dielectric constant and higher conductivity, which lead to that measured resonant frequency and 10 dB bandwidth is higher and bigger than simulated one [21], respectively. Another reason might be that the proposed antenna is implanted in the skin-mimicking gel with slight bigger than 4 mm embedded depth in the experiment. The bandwidth (BW) is calculated by:

$$BW = (VSWR-1)/(Q_T \times VSWR^{1/2}) \quad (1)$$

where Q_T and VSWR are the total quality factor and voltage standing-wave ratio, respectively. The BW presents the inversely proportional relationship to Q_T . In the body tissue, the Q_T is mainly dominated by the dielectric loss Q_d which is inversely proportional to the effective loss tangent ($\tan\delta_e$). When embedded depth is ≤ 5 mm, the $\tan\delta_e$ sharply increases to lead to reduce rapidly Q_T with increasing embedded depth [22-23]. Hence, the body tissue with high-loss properties can broaden the bandwidth of the implanted antenna. The measured operating frequencies of proposed antenna are from 280 to 540 MHz at return loss of 10 dB which is suitable for the entire Medical Device Radiocommunications Service (MedRadio) and Industrial Scientific Medical (ISM, 433–438 MHz) bands applications. The impedance matching, impedance bandwidth and radiation situation are also influenced by the superstrate. The lossy high permittivity human tissues and antenna conductors are separated by the superstrate, which restrain the leaky current from the conductor directly into the lossy materials to avoid the high permittivity human body from shorting out the antenna. Compared to the antenna without a superstrate, the stronger and more uniform distributed fields can be generated inside the human tissues and a lower SAR on the skin surface can be achieved as the implanted antenna has the superstrate layer. Higher dielectric constant of superstrate brings the lower resonant frequency. Besides, the thin superstrate layer also assists in reducing the operating frequency. Therefore, the commercially available Al₂O₃ ceramic is selected as superstrate to provide biocompatibility in this antenna because its high dielectric constant of 9.8 and low loss features satisfy the low frequency operation of an implantable antenna [24-25].

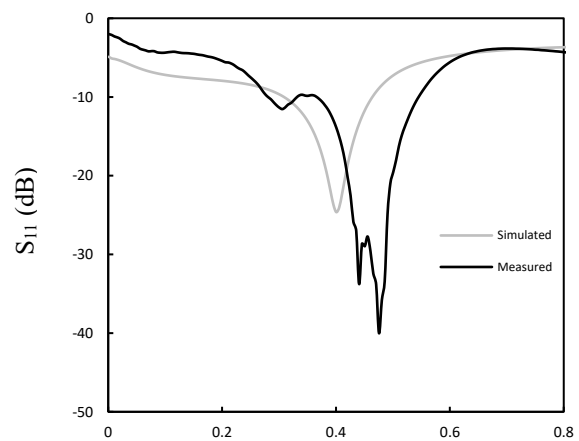


Figure 6. Measured and simulated S_{11} of the proposed implantable antenna

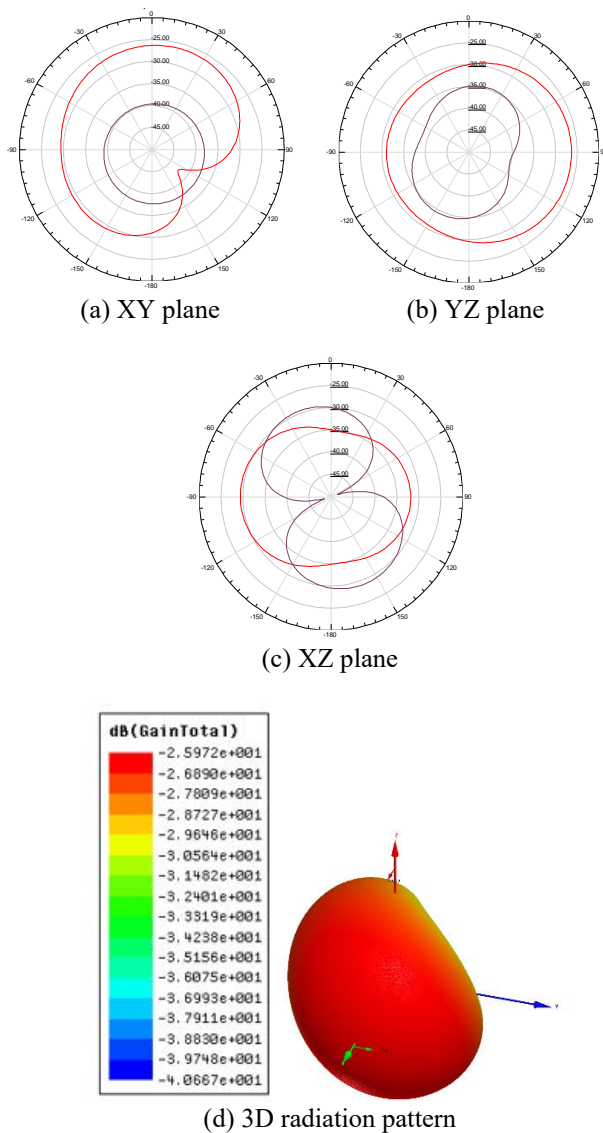


Figure 7. The radiation patterns of the proposed implantable antenna at 402 MHz: (a) XY plane, (b) YZ plane, (c) XZ plane and (d) 3D radiation pattern

The radiation patterns of the proposed implantable antenna are illustrated in Figure 7. The vertical surface current distributions of a planar monopole antenna mainly contribute the horizontal radiation patterns. If the vertical surface currents are in-phase, the planar monopole antenna could generate stronger radiation in the broadside. The H-plane radiation patterns are hard to keep omnidirectional with increasing the width of ground plane especially as width of ground plane is close to the wavelength at higher operation frequency [26]. As shown in Figure 7, it can be seen that the radiation patterns in the y-z plane are nearly omnidirectional monopole-like with low cross-polarization because of small size GL. The 3D far-field gain radiation pattern is also shown in Figure 7. A maximum peak gain of -25.9 dB can be obtained at 402 MHz because of the electrically small size and high tissue loss.

In Table 2, a detailed performance of the proposed antenna is compared one skin layer geometry implanted antennas of [11] published in the open literature in which the microstrip antenna and planar inverted-F antenna (PIFA) are designed to operate at 402–405 MHz for short-range biomedical devices application. All of three antennas in Table 2 have the similar spiral structure resonator as well as the same 4 mm implanted depth and covering 402–405 MHz. Although the dielectric constant of substrate and superstrate are lower than that of [11], the proposed antenna provides the most compact size and the largest bandwidth because bandwidth enhancement and volume reduction by a wide margin can be realized through utilizing monopole geometry and inverted-I shaped ground plane especially. The proposed implantable antenna is simulated within the simplified human model compared with [11] and measured in the human skin-mimicking gel model which closely approximates the simulated model such as size, surrounding environment, implanted depth and dielectric properties. Therefore, the measured return loss agrees well with the simulated one. Here, the proposed implantable antenna is designed without using any via or shorting pins, which can reduce the addition losses and design complexity. Results show that the proposed compact antenna with excellent performances has good potential to be used in a miniaturized implantable device.

Table 2. Comparison of implantable antennas in [6] with the proposed antenna

| Ref. | [6] | [6] | This work |
|--|---|---|---|
| Ant. resonator type | Microstrip spiral (one skin layer) | PIFA spiral (one skin layer) | Monopole spiral |
| Ant. Dimension (mm ³) | 40×36×4 | 32×24×4 | 15×15×1.42 |
| Volume (mm ³) | 5760 | 3072 | 319.5 |
| Substrate | $\epsilon_r = 10.2$ $\tan\delta = -$ | $\epsilon_r = 10.2$ $\tan\delta = -$ | FR4 $\epsilon_r = 4.4$ $\tan\delta = 0.02$ |
| Superstrate | $\epsilon_r = 10.2$ $\tan\delta = -$ | $\epsilon_r = 10.2$ $\tan\delta = -$ | Al ₂ O ₃ $\epsilon_r = 9.8$ $\tan\delta = 0.0087$ |
| Frequency | 402 MHz | 402 MHz | 402 MHz |
| -10 dB BW | Sim.: ~ 30MHz Mea.: mismatching | Sim.: ~ 30MHz Mea.: mismatching | Sim.: 150MHz Mea.: 260 MHz |
| Measured implantation scenario/ Implanted depth | Skin layer/ 4 mm | Skin layer/ 4 mm | Skin layer/ 4 mm |

4 Conclusion

In this paper, a broadband implantable antenna is presented and suitable for the Medical Device Radiocommunications Service (MedRadio) (401–406 MHz) applications. The optimal impedance matching can be obtained by properly tuning W_1 , W_2 , GW and GL . The experiment results exhibit an impedance bandwidth of 260 MHz (280–540 MHz) at return loss of 10 dB by implanting inside skin-mimicking gel. The maximum peak gain of -25.9 dB dBi is achieved at 402 MHz. The simulated and measured results confirm that the proposed antenna is a potential candidate and suitable for biomedical implantable systems.

References

- [1] X. Y. Liu, Z. T. Wu, Y. Fan, E. M. Tentzeris, A miniaturized CSRR loaded wide-beamwidth circularly polarized implantable antenna for subcutaneous real-time glucose monitoring, *IEEE Antennas and Wireless Propagation Letters*, Vol. 16, pp. 577-580, 2017.
- [2] A. Kiourt, C. W. L. Lee, J. Chae, J. L. Volakis, A wireless fully passive neural recording device for unobtrusive neuropotential monitoring, *IEEE Transactions on Biomedical Engineering*, Vol. 63, No. 1, pp. 131-137, January, 2016.
- [3] J. Lin, Y.-J. Wang, An implantable microwave antenna for interstitial hyperthermia, *Proceedings of the IEEE*, Vol. 75, No. 8, pp. 1132-1133, August, 1987.
- [4] R. Das, H. Yoo, A wideband circularly polarized conformal endoscopic antenna system for high-speed data transfer, *IEEE Transactions on Antennas and Propagation*, Vol. 65, No. 6, pp. 2816-2826, June, 2017.
- [5] A. Basir, H. Yoo, A stable impedance-matched ultrawideband antenna system mitigating detuning effects for multiple biotelemetric applications, *IEEE Transactions on Antennas and Propagation*, Vol. 67, No. 5, pp. 3416-3421, May, 2019.
- [6] S. A. A. Shah, H. Yoo, Scalp-implantable antenna systems for intracranial pressure monitoring, *IEEE Transactions on Antennas and Propagation*, Vol. 66, No. 4, pp. 2170-2173, April, 2018.
- [7] M. K. Magill, G. A. Conway, W. G. Scanlon, Tissue-independent implantable antenna for in-body communications at 2.36–2.5 GHz, *IEEE Transactions on Antennas and Propagation*, Vol. 65, No. 9, pp. 4406-4417, September, 2017.
- [8] J. Wang, Q. Wang, *Body Area Communications: Channel Modeling, Communication Systems, and EMC*, Hoboken Wiley, 2012.
- [9] N. A. Malik, P. Sant, T. Ajmal, M. Ur-Rehman, Implantable antennas for bio-medical applications, *IEEE Journal of Electromagnetics, RF and Microwaves in Medicine and Biology*, Vol. 5, No. 1, pp. 84-96, March, 2021.
- [10] G. Kaur, A. Kaur, G. K. Toor, B. S. Dhaliwal, S. S. Pattnaik, Antennas for biomedical applications, *Biomed. Eng. Lett.*, Vol. 5, pp. 203-212, September, 2015.
- [11] J. Kim, Y. Rahmat-Samii, Implanted antennas inside a human body: Simulations, designs, and characterizations, *IEEE Transactions on Microwave Theory and Techniques*, Vol. 52, No. 8, pp. 1934-1943, August, 2004.
- [12] C. Liu, Y.-X. Guo, S. Xiao, Compact dual-band antenna for implantable devices, *IEEE Antennas and Wireless Propagation Letters*, Vol. 11, pp. 1508-1511, 2012.
- [13] Z. Duan, Y. X. Guo, R. F. Xue, M. Je, D. L. Kwong, Differentially fed dual-band implantable antenna for biomedical applications, *IEEE Transactions on Antennas and Propagation*, Vol. 60, No. 12, pp. 5587-5595, December, 2012.
- [14] F. Merli, L. Bolomey, J. F. Zurcher, G. Corradini, E. Meurville, A. K. Skrivervik, Design, realization and measurements of a miniature antenna for implantable wireless communication systems, *IEEE Transactions on Antennas and Propagation*, Vol. 59, No. 10, pp. 3544-3555, October, 2011.
- [15] A. Kiourt, K. S. Nikita, Miniature scalp-implantable antennas for telemetry in the MICS and ISM bands: Design, safety considerations and link budget analysis, *IEEE Transactions on Antennas and Propagation*, Vol. 60, No. 8, pp. 3568-3575, August, 2012.
- [16] L. J. Xu, Y. X. Guo, W. Wu, Dual-band implantable antenna with open-end slots on ground, *IEEE Antennas and Wireless Propagation Letters*, Vol. 11, pp. 1564-1567, 2012.
- [17] T. Karacolak, A. Z. Hood, E. Topsakal, Design of a dual-band implantable antenna and development of skin mimicking gels for continuous glucose monitoring, *IEEE Transactions on Microwave Theory and Techniques*, Vol. 56, No. 4, pp. 1001-1008, April, 2008.
- [18] C. J. Sanchez-Fernandez, O. Quevedo-Teruel, J. Requena-Carrion, L. Inclan-Sanchez, E. Rajo-Iglesias, Dual-band microstrip patch antenna based on short-circuited ring and spiral resonators for implantable medical devices, *IET Microwaves, Antennas & Propagation*, Vol. 4, No. 8, pp. 1048-1055, August, 2010.
- [19] R. Warty, M. R. Tofighi, U. Kawoos, A. Rosen, Characterization of implantable antennas for intracranial pressure monitoring: Reflection by and transmission through a scalp phantom, *IEEE Transactions on Microwave Theory and Techniques*, Vol. 56, No. 10, pp. 2366-2376, October, 2008.
- [20] T. G. Ma, J. W. Tsai, Band-rejected ultrawideband planar monopole antenna with high frequency selectivity and controllable bandwidth using inductively coupled resonator pairs, *IEEE Transactions on Antennas and Propagation*, Vol. 58, No. 8, pp. 2747-2752, August, 2010.
- [21] N. Cho, T. Roh, J. Bae, H.-J. Yoo, A planar MICS band antenna combined with a body channel communication electrode for body sensor network, *IEEE Transactions on Microwave Theory and Techniques*, Vol. 57, No. 10, pp. 2515-2522, October, 2009.
- [22] Z. J. Yang, L. Zhu, S. Xiao, An implantable circularly polarized patch antenna design for pacemaker monitoring based on quality factor analysis, *IEEE Transactions on Antennas and Propagation*, Vol. 66, No. 10, pp. 5180-5192, October, 2018.
- [23] Z. J. Yang, L. Zhu, S. Xiao, An implantable wideband microstrip patch antenna based on high-loss property of human tissue, *IEEE Access*, Vol. 8, pp. 93048-93057, 2020.

- [24] P. Soontornpipit, C. M. Furse, Y. C. Chung, Design of implantable microstrip antenna for communication with medical implant, *IEEE Transactions on Microwave Theory and Techniques*, Vol. 52, No. 8, pp. 1944-1951, August, 2004.
- [25] M. R. Robel, A. Ahmed, A. Alomainy, W. S. T. Rowe, Effect of A Superstrate on On-Head Matched Antennas for Biomedical Applications, *Electronics*, Vol. 9, No. 7, Article No. 1099, July, 2020.
- [26] Q. Wu, R. Jin, J. Geng, M. Ding, Printed omnidirectional UWB monopole antenna with very compact size, *IEEE Transactions on Antennas and Propagation*, Vol. 56, No. 3, pp. 896-899, March, 2008.

Biographies



Ching-Fang Tseng was born in Koahsiung, Taiwan, in 1978. She received the Ph. D. degree in electrical engineering from Cheng-Kung University, Tainan, in 2007. Currently, she is a Professor in the Electronic Engineering Department at National United University, Taiwan. She

has been involved in the research and development of wearable and flexible antennas, implantable antenna, biomedical devices, microwave/mm-Wave/sub-THz mobile antennas, wireless biosensors, glass free ULTCC & LTCC microwave dielectric materials, biomedical signal analysis, nonintrusive biological signal measurement and intelligent health monitoring systems. She has author or coauthor over 100 technical publications.



Bo-Zhong Huang received the B.E degree in electronic engineering from National United University, Miaoli, Taiwan, in 2017, and is currently working toward the M.S degree in electronic engineering at the National United University. His main research direction is the development of

wireless communication substrate materials, implantable antennas and dielectric resonator antennas.



Wen-Chieh Chuang recieved the B.S. degree in electronic engineering from National United University, Miaoli, Taiwan, in 2015. His research interests include implantable antennas, wearable antennas and dielectric resonator antennas.